Electronic Theses & Dissertations (2024 - present)

The Graduate School

Fall 2024

Exploring the Epitranscriptomic Response to Senolytics and Senomorphs in Cellular Models of Aging

Emily Benson
eabenson@albany.edu

**Exploring the Epitranscriptomic Response to Senolytics and Senomorphs
in Cellular Models of Aging**

by

Emily A. Benson

A Thesis

Submitted to the University at Albany, State University of New York

in Partial Fulfillment of

the Requirements for the Degree of

Master of Science

College of Arts and Sciences

Department of Biological Sciences

2024

Acknowledgements

I would like to thank my mother and my grandmother for always pushing me to be the best person that I can possibly be. Their support, encouragement and love have gone a long way. I will always appreciate the sacrifices that they made for me throughout my life.

I would like to thank Dr. Begley for giving me the opportunity to conduct research in his lab. His mentorship and guidance have made me grow as a researcher and has made a significant impact on my academic journey. His mentorship will continue to guide me as I embark on the next chapter of my career.

I would like to thank my committee members, Dr. Melendez and Dr. Fuchs, for their insightful feedback and guidance. I would like to thank Dr. Melendez for giving me the opportunity to conduct research in his lab when I was an undergraduate student and introducing me to the senescence project.

I would like to thank our lab manager, Uli, for teaching me all the wet lab skills that I needed to learn in order to complete my project. I know I wasn't always easy to train, but she always showed up for me, and for that, I will always be grateful. Her patience and intellect helped tremendously, and I wouldn't have been able to complete this project without her.

I would like to thank Dr. Gervasi for giving me the opportunity to be a teaching assistant for her ABIO 201 and ABIO 202Z laboratory courses these past three semesters. Being a TA has helped me to further develop my communication, leadership, and problem-solving skills.

Lastly, I would like to thank my lab mates, Chetna, Humphrey, Dylan, and Aram. I'm forever grateful for being able to conduct research with such talented and hardworking individuals. I learned so much from them and am thankful for all their help, support, guidance and patience. I will forever cherish the memories that we made together in the lab. I thank them for making the lab such a friendly, welcoming and fun environment.

Table of Contents

1. Abstract

In senescence that occurs with aging, cells stop dividing and initiate a pro-inflammatory program called the senescence associated secretory phenotype (SASP). SASP can lead to cell damage and has been linked to age-related conditions such as cancer, diabetes, osteoporosis, cardiovascular disease, Alzheimer's disease, and osteoarthritis. The epitranscriptome regulates translation through post-transcriptional RNA modifications and can control when and how much of protein synthesis occurs. Several tRNA modifications that include 5-methoxycarbonylmethyl (mcm^5U), 5-methoxycarbonylmethyl-2-thiouridine (mcm^5s^2U), and mcm^5Um (5-methoxycarbonylmethyl-2′-O-methyluridine) are linked to the translation of enzymes involved in the detoxification of reactive oxygen species (ROS), and defects in these tRNA modifications have been shown to promote senescence. We examined the reprogramming of tRNA modifications in response to pharmaceuticals that limit senescence or SASP in mouse embryonic fibroblast (MEF) cells and human lung fibroblast (IMR-90) cells. These cells were treated with senolytics (Navitoclax and Quercetin) and senomorphs (Metformin and Taurine). Small RNA was purified to analyze tRNA modifications by LC-MS/MS. We have demonstrated that senolytics and senomorphs can re-program tRNA modifications in wild type mouse embryonic fibroblasts, specifically 5-methylthio-2-methyluracil (s^2mo^5U), 7-methylguanosine (m^7G), 5-methylcytosine-2-thiouridine (mcm^5s^2U), 2'-O-methylguanosine (Gm), N^1-Methyladenosine (m^1A), and 5-methoxyuridine (mo^5U). We have also demonstrated that senolytics and senomorphs can re-program tRNA modifications in senescent human lung fibroblasts, specifically 7-methylguanosine (m^7G), 1-methylguanosine (m^1G), N^2,N^2-dimethylguanosine (m^2_2G), 2-methylguanosine (m^2G), 5-methylcytosine (m^5C), N^6-methyladenosine (m^6Am), 5-methoxycarbonylmethyl (mcm^5U), 2-thiocytidine (s^2C), and

pseudouridine (Ψ), with our studies being some of the first to explore this hypothesis. Our studies highlight the potential of using senolytic and senomorphic therapeutic agents to treat tRNA-related diseases.

2. Introduction

The Central Dogma of Molecular Biology

The Central Dogma of molecular biology was first developed by Francis Crick in 1958 and proposed that genetic information flows from DNA to RNA to protein (Ostrander, 2023). During transcription, mRNA is synthesized from DNA, and during translation, mRNA codes for proteins that are synthesized at the ribosome and requires adapter molecules called tRNAs (Central Dogma of Biology, 2007). Normal RNA can be modified, where uracil (U) is modified to 5-methyluridine (m^5U), guanine (G) is modified to guanosine monophosphate (Gm), adenine (A) is modified to N^1-Methyladenosine (m^1A) or N^6-methyladenosine (m^6A), and cytosine (C) is modified to 5-methylcytosine (m^5C) (Adamopoulos et al. 2023) (**Figure 1**).

tRNA and the Epitranscriptome

A key factor of cellular senescence can be found in the epitranscriptome. There are over 170 modified nucleosides in the epitranscriptome, and these modifications can regulate stability and codon-anticodon interactions (Boo & Kim, 2020). There are 8 – 12 modifications per tRNA, and these modifications influence the stability of tRNA, the structure of tRNA, translation fidelity, and the rate of translation (Boo & Kim, 2020). The two-dimensional cloverleaf model of tRNA is comprised of three loops (Tamura, 2015) (**Figure 2**). The bottom loop is composed of anticodons, and it binds complementary to mRNA codons (Tamura, 2015) (**Figure 2**). A three-nucleotide acceptor site is present at the 3' end, which includes a free –OH group (Tamura, 2015) (**Figure 2**). Specific tRNA's will bind to specific amino acids through the acceptor stem (Tamura, 2015) (**Figure 2**). The epitranscriptome regulates translation through post-transcriptional RNA modifications and

can control when transcription occurs and how much protein synthesis occurs (Kumar & Mohapatra, 2021).

Several tRNA modifications that include 5-methoxycarbonylmethyl (mcm^{5}U), 5-methoxycarbonylmethyl-2-thiouridine (mcm^{5}s^{2}U), and mcm^{5}Um (5-methoxycarbonylmethyl-2′-O-methyluridine) are linked to the translation of enzymes involved in the detoxification of reactive oxygen species (ROS) (Endres et al. 2015). Defects in enzyme writers such as ALKBH8 (alkB homolog 8), TRMT2A (tRNA methyltransferase 2 homolog A), ELP3 (elongator complex protein 3), CTU1 (cytoplasmic tRNA 2-thiolation protein 1), and METTL1 (methyltransferase 1) have been shown to promote senescence (Puig et. al 2020). ALKBH8 is an enzyme writer for mcm^{5}U, mcm^{5}s^{2}U, and mcm^{5}Um, TRMT2A is an enzyme writer for m^{5}U, ELP3 is an enzyme writer for ncm^{5}U and mcm^{5}U, CTU1 is an enzyme writer for mcm^{5}s^{2}U, and METTL1 is an enzyme writer for m7G (Puig et. al 2020). These enzyme writers are associated with various forms of cancers, such as breast cancer, Hepatocarcinoma, and lung cancer (Puig et al. 2020). In RNA modifications, methylation is seen as a common modification. RNA methyltransferase enzymes are able to catalyze methylation through a methyl synthase mechanism, which uses the methyl donor S-adenosylmethionine (SAM) (Puig et. al 2016).

Wobble U tRNA Modifications Regulate Stress Responses

Wobble U tRNA modifications can regulate stress responses, particularly using selenocysteine (Endres et. al 2015). This is known as selenocysteine decoding, and it recodes internal UGA stop codons in mRNA (Endres et al. 2015). In order for stop codon recoding to occur, a selenocysteine insertion sequence (SECIS), located in the 3' untranslated region (UTR) of the

mRNA transcript must be present, which promotes tRNA^{SEC} into the ribosome (Endres et al. 2015).

Also, tRNA^{SEC} must contain the modified wobble uridine bases 5-methoxycarbonylmethyl (mcm^{5}U) and mcm^{5}Um (5-methoxycarbonylmethyl-2′-O-methyluridine) at position 34 (Endres et al. 2015) (**Figure 3**). These wobble uridine bases promote anticodon-codon interactions, which are necessary for the decoding of selenocysteine-containing stress response proteins, such as glutathione peroxidases (GPXs) and thioredoxin reductases (TrxRs) (Endres at el. 2015). These stress response proteins are crucial for the detoxification of reactive oxygen species (ROS) and regulating DNA damage responses (Endres et al. 2015).

Cellular Senescence

In senescence that occurs with aging, cells stop dividing, but they do not die. Over time, these senescent cells accumulate in large numbers and affect nearby tissues. As a result, these senescent cells release harmful substances and cause inflammation in nearby cells, or possibly cell death. This process is called the senescence associated secretory phenotype (SASP) (Yang et al. 2015). The SASP contains pro-inflammatory and immune-modulatory cytokines, chemokines, proteases, and growth factors (Li et al. 2023). Senescence can result in the formation of age-related conditions, such as cancer, osteoarthritis, osteoporosis, diabetes, cardiovascular disease, and Alzheimer's disease (Mylonas & O'Loghlen, 2022). The tumor suppressor and cell cycle regulator, p16^{INK4a}, is a key marker of cellular senescence and aging (Li et al. 2023). Although senescence is associated with age-related conditions, it is also vital for normal development, such as embryonic developmental, childbirth, and wound healing (Kumari & Jat, 2015). In embryonic development, senescence is

seen during tissue remodeling to prevent the spreading of damaged cells that can lead to tumor formation (Rodriguez, 2021).

In childbirth, fetal membrane senescence increases, and as a result, induces labor (Cha & Aronoff, 2017). The decidua is then activated and proinflammatory cytokines and PGs are secreted (Cha & Arronoff, 2017). This triggers a myometrial contractility pathway for labor (Cha & Arronoff, 2017). In wound healing, platelet-derived growth factor alpha polypeptide A (PDGF-A+) are produced by senescent fibroblasts in the SASP and induces wound healing (Andrade et. al 2022). Non-senescent fibroblasts are differentiated into myofibroblasts by senescent fibroblasts which results in wound contraction (Andrade et. al 2022). Senescent myofibroblasts act as a limiting factor to fibrosis through the SASP and degrades the extracellular matrix (Andrade et. al 2022). By the year 2050, it is expected that the American population who are sixty-five and older will nearly double from 48 million to 88 million (World's Older Population, 2016). Also, by 2050, the life expectancy at birth will increase globally, starting at 68.6 years in 2015, resulting to 76.2 years in 2050 (World's Older Population, 2016). With the increase of life expectancy, there will be a greater need for treatments for age-related diseases.

Senolytics and Senomorphics

Certain agents such as senolytics and senormorphs have been proven to eliminate the onset of senescent-related diseases. Senolytics eliminate senescent cells by inducing apoptosis of senescent cells (Kirkland & Tchkonia, 2020). Senolytic drugs include Dasatinib, Quercetin, Navitoclax, and Fisetin (Kirkland & Tchkonia, 2020). Senomorphs suppress pathological SASPs and causes senostasis without inducing apoptosis (Zhang et. al 2022). Senomorphs include Rapamycin, Metformin, Resveratrol, and Aspirin (Zhang et. al 2022). Navitoclax (ABT-

263), an anti-cancer drug that can treat small cell lung cancer and acute lymphocytic leukemia, is a Bcl-2 family protein inhibitor that binds to apoptotic effectors of the proteins Bax and Bak, which can lead to apoptosis in tumor cells that overexpress Bcl-2, Bcl-XL, and Bcl-w (Vos et. al 2020). Navitoclax is not FDA approved, but it is currently undergoing Phase 3 clinical trials (Dilley et. al 2020). Quercetin is a plant pigment called a flavonoid and is found in fruits and vegetables such as onions, grapes, berries, cherries, broccoli, and citrus fruits (David et. al, 2016). It has been shown that flavonoids limit age-related conditions such as cardiovascular disease, metabolic disorders, and certain types of cancer by decreasing oxidative stress (David et. al, 2016). Quercetin can induce apoptosis by upregulating Bax, caspase-3, and p21 while downregulating Akt, PLK-1, cyclin-B1, cyclin-A, CDC-2, CDK-2, and Bcl-2 (Sethi et al. 2023). Metformin is an antidiabetic agent used to treat type II diabetes mellitus (Corcoran & Jacobs, 2022). Metformin inhibits the expression of genes that code for inflammatory cytokines during cellular senescence and has been shown to inhibit the growth of certain cancer cells (Moiseeva et al. 2013). Metformin is able to reduce SASP by interfering with IKK/NF-κB activation, resulting in the inhibition of the mTOR and stat3 pathways (Hu et al. 2020). Taurine is an amino acid found in the human body, naturally in foods that are high in protein, such as meat and fish, and in certain energy drinks (Schaffer & Kim, 2018). Taurine is made from cysteine and hypotaurine, and it works as a neurotransmitter in the brain (Schaffer & Kim, 2018). It can also be used a therapeutic agent against heart failure and was approved for the treatment of congestive heart failure in Japan (Schaffer & Kim, 2018). Not only is Taurine effective in treating heart failure, but it studies have shown that it can be affective in treating mitochondrial-related diseases. ROS generated by the mitochondria damages antioxidant enzymes that are crucial in preventing oxidative stress, but Taurine might limit oxidative stress

by the mitochondrial electron transport chain through its anti-inflammatory activity with the formation of N-chlorotaurine (Baliou et al. 2021). The conjugation of Taurine to the tRNA also plays a crucial role in limiting oxidative stress.

Little is known as to how tRNA modifications are affected by senolytic and senomorphic treatments. To examine this, WT MEFs were treated with navitoclax, quercetin, metformin and taurine, and senescent IMR-90 fibroblasts were treated with navitoclax. Small RNA purification was performed to analyze tRNA modifications using LC-MS/MS liquid chromatography-mass spectrometry (LC-MS/MS). LC-MS/MS analysis demonstrated that senolytics and senomorphs can re-program tRNA modifications, such as 7-methylguanosine (m^7G), N^1-Methyladenosine (m^1A), and 5-methoxyuridine (mo^5U)

3. Materials and Methods

Cell Culture:

Mouse embryonic fibroblasts were cultured in Dulbecco's Modified Eagle's Medium - high glucose (Sigma – Aldrich, Darmstadt, Germany, catalog no. D6429) with 10% total volume of Fetal Bovine Serum (Sigma - Aldrich, Darmstadt, Germany, catalog no. F4135), 1mM in final volume of MEM Non-Essential Amino Acids Solution (100X) (Gibco, catalog no. 11140-050), and 1X in total volume of Pen Strep (Gibco, catalog no. 15140-122). All experiments were conducted at passage 7.

IMR-90 fibroblasts were cultured in Eagle's Minimum Essential Medium (Sigma – Aldrich, Darmstadt, Germany, catalog no. M4655) with 10% total volume of Fetal Bovine Serum (Sigma - Aldrich, Darmstadt, Germany, catalog no. F4135), 1mM in final volume of Sodium Pyruvate (100X) (Gibco, catalog no. 11360-070), and 1X in total volume of Pen Strep (Gibco, catalog no. 15140-122). Senescence was induced by replicative senescence, and all experiments were conducted at passage 16.

Cell Viability Assay (WT MEFs):

1. 50,000 mouse embryonic fibroblasts were seeded at passage 7 per well in 12-well plates for 24 hours and incubated at 37 °C, 5% CO_2.

2. 24 hours later, cells were treated in 1mL of medium per well that did not contain FBS or Pen Strep with each senolytic and senomorph with its corresponding control. DMSO (Thermo Fisher Scientific, catalog no. BP2311) was used as a control for navitoclax (Adooq Biosciences, catalog no. A10022) and quercetin (received from the Berglund Lab

at the RNA Institute, University at Albany, SUNY), PBS (Sigma-Aldrich, catalog no. D8537-500ML) was used as a control for metformin (Adooq Bioscience, catalog no. A10573), and media was used as a control for taurine (Thermo Fisher Scientific, catalog no. A12403.22). Navitoclax: 6.25, 12.5, 25, 50, 100, 200, and 400 uM. Quercetin: 25, 50, 100, 200, 300, 400, 500 uM, Metformin: 25, 50, 100, 200, 300, 400, 500, and 800 mM, and Taurine: 40 mM, 440 mM). The cells were treated for 1 hour and incubated at 37 °C, 5% CO_2.

3. 1 hour later, the medium was aspirated and replaced with 1 mL of medium that contained FBS and Pen Strep. The cells were then incubated at 37 °C, 5% CO_2 for 24 hours.

4. 24 hours later, the cells were detached using 200 ul of trypsin and centrifuged at 1000 RPM for 5 minutes at 24 °C. The medium was aspirated, and the pellet was resuspended in 100 ul of medium.

The cells were then counted using the trypan blue exclusion method to generate a dose response curve.

Cell Viability Assay (Senescent IMR-90's):

1. 45,000 senescent IMR-90 fibroblasts were seeded at passage 16 per well in 12-well plates for 24 hours and incubated at 37 °C, 5% CO_2.

2. 24 hours later, cells were treated in 1mL of medium per well that did not contain FBS or Pen Strep with navitoclax and DMSO at 5, 10, 15, 25, 35, 45, and 50 uM. The cells were treated for 1 hour and incubated at 37 °C, 5% CO_2.

3. 1 hour later, the medium was aspirated and replaced with 1 mL of medium that contained FBS and Pen Strep. The cells were then incubated at 37 °C, 5% CO_2 for 24 hours.

4. 24 hours later, the cells were detached using 200 ul of trypsin and centrifuged at 1000 RPM for 5 minutes at 24 °C. The medium was aspirated, and the pellet was resuspended in 100 ul of medium. The cells were then counted using the trypan blue exclusion method to generate a dose response curve.

Lethal Dose Calculations:

The LD4 and LD20 values were calculated using GraphPad Prism's online lethal dose calculator (https://www.graphpad.com/quickcalcs/Ecanything1.cfm).

RNA Extraction (WT MEFs):

1. 725,000 WT MEFs were seeded on 100 mm cell culture dishes and incubated for 24 hours at 37 °C, 5% CO_2.

2. 24 hours later, cells were treated in 10 mL of medium per dish that did not contain FBS or Pen Strep with the corresponding LD4 and LD20 values of each senolytic and senomorph, as well as its corresponding control.

3. 1 hour later, the medium was aspirated and replaced with 10 mL of medium that contained FBS and Pen Strep. The cells were then incubated at 37 °C, 5% CO_2 for 24 hours.

4. 24 hours later, 1 mL of TriZOL was added directly to the surface of the dishes for 5 minutes to lyse the cells. After 5 minutes, the surface of the dishes were "washed" with the TRIzol (Invitrogen by Thermo Fisher Scientific, catalog no. 15596018) and collected in 1.5 mL microcentrifuge tubes.

5. 200 uL of chloroform (Sigma-Aldrich, catalog no. C2432-1L) was added to each 1.5 mL microcentrifuge tube. After the chloroform was added, the microcentrifuge tubes were shaken vigorously by hand for 15 seconds and vortexed for 5 seconds.

6. After the microcentrifuge tubes were vortexed, they were incubated at room temperature for 3 minutes to separate the solution into the aqueous and organic phase.

7. After 3 minutes, the microcentrifuge tubes were centrifuged at 14,000 RPM for 15 minutes at 4 °C.

8. After 15 minutes of centrifugation, 400 ul of the upper aqueous phase was collected. Small RNA was purified using the Invitrogen PureLink miRNA Isolation Kit (Thermo Fisher Scientific, catalog no. K157001), and total RNA was purified using the Invitrogen PureLink RNA Mini Kit (Thermo Fisher Scientific, catalog no. 12183018A).

RNA Extraction (Senescent IMR-90s):

1. 1,000,000 senescent IMR-90 fibroblasts were seeded on T-175 cell culture flasks and incubated for 24 hours at 37 °C, 5% CO_2.

2. 24 hours later, cells were treated in 30 mL of medium per flask that did not contain FBS or Pen Strep with the corresponding LD4 and LD20 values of Navitoclax, as well as the corresponding control.

3. 1 hour later, the medium was aspirated and replaced with 30 mL of medium that contained FBS and Pen Strep. The cells were then incubated at 37 °C, 5% CO_2 for 24 hours.

4. 24 hours later, 1 mL of TriZOL was added directly to the surface of the flasks for 10 minutes to lyse the cells. After 10 minutes, the surface of the flasks were "washed" with the TRIzol and collected in 1.5 mL microcentrifuge tubes.

5. 200 uL of chloroform was added to each 1.5 mL microcentrifuge tube. After the chloroform was added, the microcentrifuge tubes were shaken vigorously by hand for 15 seconds and vortexed for 5 seconds.

6. After the microcentrifuge tubes were vortexed, they were incubated at room temperature for 3 minutes to separate the solution into the aqueous and organic phase.

7. After 3 minutes, the microcentrifuge tubes were centrifuged at 14,000 RPM for 15 minutes at 4 °C.

8. After 15 minutes of centrifugation, 400 ul of the upper aqueous phase was collected. Small RNA was purified using the Invitrogen PureLink miRNA Isolation Kit (Thermo Fisher Scientific, catalog no. K157001), and total RNA was purified using the Invitrogen PureLink RNA Mini Kit (Thermo Fisher Scientific, catalog no. 12183018A).

RNA Integrity Analysis:

RNA integrity was examined using the Nanodrop. It was also examined using the Agilent Bioanalyzer in the Microarray Core Facility, located at the RNA Institute at the University at Albany, SUNY.

Liquid Chromatography Mass Spectrometry Analysis:

To examine tRNA modifications, 100 ng of WT MEF small RNA samples and 300 ng of senescent small RNA samples were digested and submitted for LC-MS/MS analysis at The RNA Epitranscriptomics and Proteomics Resources (REPR), located at the University at Albany, SUNY. Sample digestion was conducted using REPR's protocol

(file:///C:/Users/benso/Downloads/Epitranscriptomics_%20Lab%20Protocol_Final%20Print_QL _20190307[1][7]%20(2).pdf).

tRNA Modification Analysis:

tRNA modification analysis was conducted using GraphPad Prism, specifically the unpaired parametric t-test. The threshold for the p-value comparisons was set to 0.1.

RT-qPCR (Senescent IMR-90s):

RT-qPCR was conducted using SYBR Green on the QuantStudio 3 Real-Time PCR System (Thermo Fisher Scientific, catalog no. A26336). 100 ng of cDNA was used. Protocol for a 10 ul reaction:

	1 Rxn
Power SYBR Green RT PCR Mix (2x)	5
Forward Primer (10 µM)	0.2
Reverse Primer (10 µM)	0.2
RT Enzyme Mix (125X)	0.08
RNA template (100 ng/uL)	0.5
RNase-Free Water	4.02

The Power SYBR Green RT-PCR Mix and the RT Enzyme Mix were purchased from Thermo Fisher Scientific (catalog no. 4389986). IL-6 and IL-8 primers were received from the Melendez Lab at the University at Albany, College of Nanoscale Science and Engineering.

Forward primer for IL-6: 5'-CCA-CAC-AGA-CAG-CCA-CTC-ACC-3'.

Reverse primer for IL-6: 5'-CTA-CAT-TTG-CCG-AAG-AGC-CCT-C-3'.

 Forward primer for IL-8: 5'-CTC-TCT-TGG-CAG-CCT-TCC-TGA-TT-3'.

Reverse primer for IL-8: 5'-AAC-TTC-TCC-ACA-ACC-CTC-TGC-AC-3'.

RT-qPCR Analysis:

RT-qPCR analysis was conducted using GraphPad Prism, specifically the unpaired parametric test. The threshold for the p-value comparisons was set to 0.05. The ΔCT values were calculated using the formula $\Delta CT = CT$ (target gene) – CT (reference gene). The $\Delta\Delta CT$ values were calculated using the formula $\Delta\Delta CT = \Delta CT$ (target sample) - ΔCT (reference sample). The relative fold change was calculated using the formula $2^{-\Delta\Delta ct}$.

4.Results and Discussion

Dose Response Curves:

The results of the dose response curves are shown in figures 4A through 4D. Navitoclax has a LD_4 value of 1.25 uM and a LD_{20} value of 11.69 uM (**Figure 4A**), quercetin has a LD_4 value of 9.55 uM and a LD_{20} value of 59.81 uM (**Figure 4B**), and metformin has a LD_4 value of 71.90 mM and a LD_{20} value of 169.89 mM (**Figure 4C**). Navitoclax has a LD_4 value of 2.18 uM and a LD_{20} value of 6.37 uM (**Figure 4D**).

m^7G Decreases in Response to the LD_{20} Treatment of Navitoclax, $mcms^2U$ Increases in Response to the LD_{20} Treatment of Navitoclax, and s^2mo^5U Increases in Response to the LD_4 Treatment of Navitoclax in WT MEFs. tRNA modifications of WT MEFs treated with the LD_{20} values of navitoclax, along with the control (DMSO) were analyzed using LC-MS/MS. The unpaired parametric t-test analysis showed there was a significance in m^7G between the navitoclax treated group and the control group (DMSO) (p = 0.024263) (**Figure 5A**) (**Figure 10**). The unpaired parametric t-test analysis showed there was a significance in mcm^5s^2U between the navitoclax treated group and the control group (DMSO) (p = 0.065339) (**Figure 5B**) (**Figure 10**). The unpaired parametric

t-test analysis showed there was a significance in s^2mo^5U between the navitoclax treated group and the control group (DMSO) (p = 0.005415) (**Figure 5C**) (**Figure 10**).

Gm and m^1A Decrease in Response to the LD_{20} Treatment of Quercetin in WT MEFs. tRNA modifications of WT MEFs treated with the LD_{20} values of quercetin, along with the control (DMSO) were analyzed using LC-MS/MS. The unpaired parametric t-test analysis showed there was a significance in Gm between the quercetin treated group and the control group (DMSO) (p = 0.097504) (**Figure 6A**) (**Figure 10**). The unpaired parametric t-test analysis showed there was a significance in m^1A between the Quercetin treated group and the control group (DMSO) (p = 0.027524) (**Figure 6B**) (**Figure 10**).

Gm and mo^5U Increase in Response to the LD_4 Treatment of Metformin in WT MEFs. tRNA modifications of WT MEFs treated with the LD_4 values of Metformin, along with the control (PBS) were analyzed using LC-MS/MS. The unpaired parametric t-test analysis showed there was a significance in Gm between the Metformin treated group and the control group (PBS) (p = 0.88512) (**Figure 7A**) (**Figure 10**). The unpaired parametric t-test analysis showed there was a significance in mo^5U between the Metformin treated group and the control group (PBS) (p = 0.022883) (**Figure 7B**) (**Figure 10**).

No Significance in tRNA Modifications in 40 mM and 440mM Treatments of Taurine in WT MEFS. tRNA modifications of WT MEFs treated with 40 mM and 440 mM of taurine, along with the control (media) were analyzed using LC-MS/MS. The unpaired parametric t-test analysis showed there was insignificance in both the 40 mM and 440 mM treatments (**Figure 10**).

m^{7}G Decreases in Response to the LD$_4$ Treatment of Navitoclax in Senescent IMR-90s.

tRNA modifications of senescent IMR-90 fibroblasts were treated with the LD$_4$ values of

navitoclax, along with the control (DMSO) were analyzed using LC-MS/MS. The unpaired

parametric t-test analysis showed there was a significance in m^{7}G between the Navitoclax

treated group and the control group (DMSO) (p = 0.059274) (**Figure 8**) (**Figure 10**).

m^{1}G, m$^2_2$G, m^{2}G, m^{5}C, m^{6}Am, mcm^{5}U, s^{2}C, and Y Increase in Response to the LD$_{20}$ Treatment of Navitoclax in Senescent IMR-90s. tRNA modifications of senescent IMR-90 fibroblasts were treated with the LD$_{20}$ values of navitoclax, along with the control (DMSO) were analyzed using LC-MS/MS. The unpaired parametric t-test analysis showed there was a significance in m^{1}G between the navitoclax treated group and the control group (DMSO) (p = 0.091307) (**Figure 9A**) (**Figure 10**). The unpaired parametric t-test analysis showed there was a significance in m$^2_2$G between the navitoclax treated group and the control group (DMSO) (p = 0.08819) (**Figure 9B**) (**Figure 10**). The unpaired parametric t-test analysis showed there was a significance in m^{2}G between the navitoclax treated group and the control group (DMSO) (p = 0.105999) (**Figure 9C**) (**Figure 10**). The unpaired parametric t-test analysis showed there was a significance in m^{5}C between the navitoclax treated group and the control group (DMSO) (p = 0.059216) (**Figure 9D**) (**Figure 10**). The unpaired parametric t-test analysis showed there was a significance in m^{6}Am between the navitoclax treated group and the control group (DMSO) (p = 0.08901) (**Figure 9E**) (**Figure 10**). The unpaired parametric t-test analysis showed there was a significance in mcm^{5}U between the navitoclax treated group and the control group (DMSO) (p = 0.049288) (**Figure 9F**) (**Figure 10**). The unpaired parametric t-test analysis showed there was a significance in s^{2}C between the navitoclax treated group and the control group (DMSO) (p = 0.093184) (**Figure 9G**) (**Figure 10**). The unpaired parametric t-test analysis showed there was a significance in Y between the navitoclax treated group and the control group (DMSO) (p = 0.036649) (**Figure 9H**) (**Figure 10**).

LD$_4$ Treatment of Navitoclax Upregulates IL-8 Expression in Senescent IMR-90's. Since

the pro-inflammatory cytokine IL-8 is highly expressed in the SASP, we examined whether the

LD$_4$ and LD$_{20}$ treatments of navitoclax in senescent IMR-90's affects IL-8 expression. SYBR

Green qPCR was conducted using 100 ng of cDNA. The relative fold change was calculated

using the formula $2^{-\Delta\Delta ct}$. The unpaired parametric t-test showed there was significance in the LD$_4$

(p = 0.04), but not the LD$_{20}$ (p = 0.13) (**Figures 11A and 11B**).

LD$_4$ and LD$_{20}$ Treatment of Navitoclax does not Affect IL-6 Expression in Senescent IMR-90's. Since the pro-inflammatory cytokine IL-6 is highly expressed in the SASP, we examined whether the LD$_4$ and LD$_{20}$ treatments of navitoclax in senescent IMR-90's affects IL-6 expression. SYBR Green qPCR was conducted using 100 ng of cDNA. The relative fold change was calculated using the formula $2^{-\Delta\Delta ct}$. The unpaired parametric t-test showed there was insignificance in the LD$_4$ (p = 0.7212) (9A) and LD$_{20}$ (p = 0.8077) (**Figures 12A and 12B**).

5.Conclusion

Our studies highlight the reprogramming of tRNA modifications when treated with the LD$_4$ and LD$_{20}$ values of navitoclax, quercetin, and metformin in wild type mouse embryonic fibroblasts, as well as the LD$_4$ and LD$_{20}$ treatment of navitoclax in senescent human lung (IMR-90) fibroblasts. A wild type cell model was used to compare a senescent cell model. Toxic doses were used (LD$_4$ and LD$_{20}$) as opposed to pharmaceutical doses because we wanted to achieve a significant biological effect. Using a pharmaceutical dose might not have shown significant changes in tRNA modifications compared to a toxic dose. Previous studies have examined the reprogramming of mRNA modifications in response to senolytic and senomorphic treatments. Previous studies have shown that quercetin decreases mRNA modification m^{6}A and its corresponding writer, METTL3, in insulin resistant, skeletal muscle of C57Bl/6 mice (Jiao et al. 2022). Previous studies have shown that Gm decreases in patients with colorectal cancer (Zheng et. al 2023). Our studies show that m^{1}A and Gm decrease in response to the LD$_{20}$ treatment of quercetin in wild type mouse embryonic fibroblasts. Previous studies have shown that decreased levels of the mRNA modification m^{1}A promotes hepatocellular carcinoma (Wu

et. al 2024). Previous studies have also shown that in human breast cancer cells, metformin is able to decrease m^6A by decreasing METTL3 expression mediated by miR-483-3p (Cheng et al. 2021). In previous studies, METTL3 was shown to regulate m^6A in stress responses, and METTL3 and m^6A were found to be upregulated in cancer cells, such as colorectal cancer (Sun et. al 2023). Our studies show that mo^5U increases in response to the LD_4 treatment of metformin in wild type mouse embryonic fibroblasts. mo^5U is located in tRNA^{Thr} from gram-positive bacteria, such as Bacillus subtilis (Sakai et. al 2019). The link between mo^5U and senescence is still unknown. Our studies also show that m^7G decreases in response to the LD_{20} treatment of navitoclax in wild type mouse embryonic fibroblasts and senescent human lung fibroblasts. METTL1 is a writer for m^7G, and it has been shown to regulate the initiation and progression of tumors through m^7g methylation (Cheng et. al 2022). METTL1 has also been shown to be overexpressed in cancers, such as bladder cancer (Ying et. al 2021). ALKBH8 is a tRNA methyltransferase that methylates the wobble uridine of mcm^5U (Songe-Moller et. al 2010). ALKBH8 catalyzes the conversion of mcm^5U to mcm^5s^2U by the addition of a sulfur atom to the 2-position of the uridine base (Songe-Moller et. al 2010). In mice, prior ALKBH8-mediated methylation is required for the thiolation and 2′-O-ribose methylation that form 5-methoxycarbonylmethyl-2-thiouridine (mcm^5s^2U) and 5-methoxycarbonylmethyl-2′-O-methyluridine (mcm^5Um), and these specific thiolation and ribose methylation enzymes use mcm^5U as a substrate (Songe-Moller et. al 2010). In ALKBH8 deficient mice, it has been shown that ALKBH8 deficient mice lack mcm^5U, mcm^5Um, and mcm^5s^2U in total tRNA (Songe-Moller et. al 2010). Although the ALKBH8 deficient mice appeared to be normal despite their loss of these uridine modifications, the selenocysteine-specific tRNA (tRNA^{Sec}) was modified and the selenoprotein Gpx1 caused reduced recoding of the UGA stop codon to selenocysteine (Songe-

Moller et. al 2010). The ribose methylation of mcm^{5}U in tRNA^{Sec} regulates selenoprotein synthesis, and selenoproteins, such as glutathione peroxidase 1 (Gpx1), are promoted by mcm^{5}Um-containing tRNA^{Sec} (Songe-Moller et. al 2010). ALKBH8 deficiency can alter selenoprotein levels, resulting in an imbalance of reactive oxygen species (Lee et. al 2020). Imbalance of reactive oxygen species promotes senescence (Lee et. al 2020). Our studies show that mcm^{5}s^{2}U is increases when wild type mouse embryonic fibroblasts are treated with the LD$_{20}$ of navitoclax. Our studies also show that mcm^{5}U is upregulated when senescent human lung fibroblasts are treated with the LD$_{20}$ of navitoclax. Lastly, in wild type mouse embryonic fibroblasts, we show that s2mo5U increases when treated with the LD$_{20}$ of navitoclax. In senescent human lung fibroblasts, we also show that m^{1}G, m$^2_2$G, m^{2}G, m^{5}C, m^{6}Am, s^{2}C, and Ψ increase in response to the LD20 treatment of navitoclax. Previous studies have shown that a decrease in the mRNA modification m^{1}G in human serum might be associated with breast cancer, and a decrease in the mRNA modification m^{2}G was found in patients with colorectal cancer (Zheng et. al 2023). TRMT1, the writer for m$^2_2$G, can cause neurological disorders in humans when it experiences loss-of-function mutations (Xiong et. al 2023). Lastly, both m^{5}C and Ψ regulate cellular stress responses, and reprogramming of their writers, erasers and readers have been linked to cancer (Nombela et. al 2021). Ψ may serve as a potential biomarker for certain cancers, since it has been found to be highly detected in the urine of colon, prostate, and ovarian cancer patients (Nombela et. al 2021). Since the pro-inflammatory cytokines IL-6 and IL-8 are highly expressed in the SASP, we hypothesized that treating wild type mouse embryonic fibroblasts with the LD$_4$ and LD$_{20}$ values of navitoclax would downregulate IL-6 and IL-8 expression. In previous studies, navitoclax downregulated IL-6 expression in cancer-associated fibroblasts, compared to quercetin and dasatanib which

upregulated IL-6 expression (Bogdanova et al. 2024). In our studies, navitoclax upregulated IL-8 expression and had no effect on IL-6 expression. It's important to note cell type and the method of senescence induction might influence differences in metabolic, transcriptional, and SASP profiles (Bogdanova el at. 2024). Therefore, certain senolytics might not be an ideal treatment for certain types of cells and certain age-related conditions. Furthermore, by reprogramming the epitranscriptome, our studies highlight the potential of using senolytics and senomorphs as therapeutic agents to treat age-related diseases. By potentially improving stress responses and modulating cellular senescence, this might be able to limit the effects of aging at the cellular level. Further studies are needed to study the specific mechanisms of how senolytics and senomorphs can reprogram certain tRNA modifications.

6.Future Directions

In the future, we would like to compare wild type mouse embryonic fibroblasts to senescent mouse embryonic fibroblasts when treated with the LD_4 and LD_{20} values of navitoclax, quercetin, metformin, and taurine. We would also like to test different treatment times since in our studies, we only conducted one hour of treatment. We would also like to test more senolytics and senomorphs, such as dasatinib and rapamycin since they have been shown to be a potential therapeutic agent for certain age-related conditions. We would also like to compare non-senescent IMR-90 fibroblasts to senescent IMR-90 fibroblasts when treated with the LD_4 and LD_{20} values of navitoclax, quercetin, metformin, and taurine. In our studies, we only examined senescent IMR-90 fibroblasts when treated with the LD_4 and LD_{20} values of navitoclax. We would like to examine IL-6 and IL-8 expression in non-senescent IMR-90 fibroblasts when treated with the LD_4 and LD_{20} values of navitoclax since we only examined

senescent IMR-90 fibroblasts. Lastly, we would like to examine the effect of navitoclax treatment on ALKBH8 and selenoprotein expression in wild type mouse embryonic fibroblasts, ALKBH8 deficient mouse embryonic fibroblasts, and senescent human lung fibroblasts.

7.Appendix Materials

All raw and processed RNA modification data, as well as supplemental data/figures can be

found in the Dropbox folder.

https://www.dropbox.com/scl/fo/ejb9hkwmtol8uma3llxn2/AOKJs7WpRbqqCdOe6Z8HwB4?rlkey

=fx08i75g3otntdbjhvzlk878j&st=1p0n6fej&dl=0

8.References

Boo, S. H., & Kim, Y. K. (2020, March 24). *The emerging role of RNA modifications in the regulation of mrna stability*. Nature News. Retrieved April 10, 2023, from https://www.nature.com/articles/s12276-020-0407-z

Endres, L., Begley, U., Clark, R., Gu, C., Dziergowska, A., Małkiewicz, A., Melendez, J. A., Dedon, P. C., & Begley, T. J. (2015, July 6). *ALKBH8 regulates selenocysteine-protein expression to protect against reactive oxygen species damage*. PloS one. Retrieved April 10, 2023, from https://www.ncbi.nlm.nih.gov/pmc/articles/PMC4492958/

Kirkland, J. L., & Tchkonia, T. (2020, July 19). *Senolytic drugs: From Discovery to translation*. Wiley Online Library. Retrieved April 11, 2023, from https://onlinelibrary.wiley.com/doi/10.1111/joim.13141

Kumar, S., & Mohapatra, T. (2021, April 19). Dynamics of DNA methylation and its functions in plant growth and development. Frontiers. Retrieved April 10, 2023, from https://www.frontiersin.org/articles/10.3389/fpls.2021.596236/full

Mylonas, A., & O'Loghlen, A. (2022, February 28). Cellular senescence and ageing: Mechanisms and interventions. Frontiers. https://www.frontiersin.org/articles/10.3389/fragi.2022.866718/full

U.S. Department of Health and Human Services. (2016, March 28). World's older population grows dramatically. National Institutes of Health. https://www.nih.gov/news-events/news-releases/worlds-older-population-grows-dramatically

Yang, H., Chen, C., Chen, H., Duan, X., Li, J., Zhou, Y., Zeng, W., & Yang, L. (2020, July 1). Navitoclax (ABT263) reduces inflammation and promotes chondrogenic phenotype by clearing senescent osteoarthritic chondrocytes in osteoarthritis. National Library of Medicine. https://www.ncbi.nlm.nih.gov/pmc/articles/PMC7377880/

Zhang, L., Pitcher, L. E., Prahalad, V., Niedernhofer, L. J., & Robbins, P. D. (2022, January 11). Targeting cellular senescence with senotherapeutics: senolytics and senomorphics. Febs Press. https://febs.onlinelibrary.wiley.com/doi/abs/10.1111/febs.16350

Adamopoulos, P. G., Athanasopoulou, K., Daneva, G. N., & Scorilas, A. (2023b, January 25). The repertoire of RNA modifications orchestrates a plethora of cellular responses. International journal of molecular sciences. https://www.ncbi.nlm.nih.gov/pmc/articles/PMC9916637/

Kumari, R., & Jat, P. (2021, February 16). Mechanisms of cellular senescence: Cell cycle arrest and senescence associated secretory phenotype. Frontiers. https://www.frontiersin.org/articles/10.3389/fcell.2021.645593/full#:~:text=Senescence%20plays%20key%20physiological%20roles,cells%20(Helman%20et%20al.%2C

Tamura, K. (2015, December 3). Origins and early evolution of the trna molecule. Life (Basel, Switzerland). https://www.ncbi.nlm.nih.gov/pmc/articles/PMC4695843/

Sandy, D. (2019, September 26). Selenoprotein P in insulin resistance. BBC. https://betterbodychemistry.com/ir/selenoprotein-insulin-resistance/

Esteve-Puig, R., Bueno-Costa, A., & Esteller, M. (2020, January 25). Writers, readers and erasers of RNA modifications in cancer . ScienceDirect. https://www.sciencedirect.com/science/article/pii/S0304383520300355

Labunskyy, V. M., Hatfield, D. L., & Gladyshev, V. N. (2014, July). Selenoproteins: Molecular pathways and physiological roles. Physiological reviews. https://www.ncbi.nlm.nih.gov/pmc/articles/PMC4101630/

de Mera-Rodríguez, J. A., Álvarez-Hernán, G., Gañán, Y., Martín-Partido, G., Rodríguez-León, J., & Francisco-Morcillo, J. (2021, January 5). Is senescence-associated β-galactosidase a reliable in vivo marker of cellular senescence during embryonic development?. Frontiers. https://www.frontiersin.org/articles/10.3389/fcell.2021.623175/full

Cha, J. M., & Aronoff, D. M. (2017). A role for cellular senescence in birth timing. Cell cycle (Georgetown, Tex.). https://www.ncbi.nlm.nih.gov/pmc/articles/PMC5731422/#:~:text=It%20has%20been%20proposed%20that,via%20increased%20fetal%20membrane%20senescence.&text=This%20process%20is%20thought%20to,towards%20myometrial%20contractility%20for%20labor.

Andrade, A. M., Sun, M., Gasek, N. S., Hargis, G. R., Sharafieh, R., & Xu, M. (2022, November 29). Role of senescent cells in cutaneous wound healing. MDPI. https://www.mdpi.com/2079-7737/11/12/1731

de Vos, S., Leonard, J. P., Friedberg, J. W., Zain, J., Dunleavy, K., Humerickhouse, R., Hayslip, J., Pesko, J., & Wilson, W. H. (2021). Safety and efficacy of navitoclax, a BCL-2 and BCL-X_L inhibitor, in patients with relapsed or refractory lymphoid malignancies: results from a phase 2a study. *Leukemia & lymphoma*, *62*(4), 810–818. https://doi.org/10.1080/10428194.2020.1845332

Dilley, K., Harb, J., Jalaluddin, M., Hutti, J. E., & Potluri, J. (2020). A Phase 3, Open-Label, Randomized Study Evaluating the Efficacy and Safety of Navitoclax Plus Ruxolitinib Versus Best Available Therapy in Patients with Relapsed/Refractory Myelofibrosis (TRANSFORM-2). *Blood*, *136*(Supplement 1), 8–8. https://doi.org/10.1182/blood-2020-139247

Anand David, A. V., Arulmoli, R., & Parasuraman, S. (2016). Overviews of biological importance of quercetin: A bioactive flavonoid. Pharmacognosy reviews. https://www.ncbi.nlm.nih.gov/pmc/articles/PMC5214562/

Corcoran, C., & Jacobs, T. F. (2022, May 22). National Center for Biotechnology Information. National Library of Medicine. https://www.ncbi.nlm.nih.gov/books/NBK518983/

Moiseeva, O., Deschenes-Simard, X., St-Germain, E., Igelmann, S., Huot, G., Cadar, A. E., Bourdeau, V., Pollak, M. N., & Ferbeyre, G. (2013, April 23). Metformin inhibits the senescence-associated secretory phenotype by interfering with IKK/NF-KB activation. PubMed. https://pubmed.ncbi.nlm.nih.gov/23521863/

Sethi, G., Rath, P., Chauhan, A., Ranjan, A., Choudhary, R., Ramniwas, S., Sak, K., Aggarwal, D., Rani, I., & Tuli, H. S. (2023). Apoptotic Mechanisms of Quercetin in Liver Cancer: Recent Trends and Advancements. *Pharmaceutics*, *15*(2), 712. https://doi.org/10.3390/pharmaceutics15020712

Hu, Qinchao, et al. "Metformin as a Senostatic Drug Enhances the Anticancer Efficacy of CDK4/6 Inhibitor in Head and Neck Squamous Cell Carcinoma." *Cell Death & Disease*, vol. 11, no. 10, 28 Oct. 2020, https://doi.org/10.1038/s41419-020-03126-0. Accessed 2 May 2022.

Schaffer, S., & Kim, H. W. (2018). Effects and Mechanisms of Taurine as a Therapeutic Agent. *Biomolecules & therapeutics*, *26*(3), 225–241. https://doi.org/10.4062/biomolther.2017.251

Baliou, S., Adamaki, M., Ioannou, P., Pappa, A., Panayiotidis, M. I., Spandidos, D. A., Christodoulou, I., Kyriakopoulos, A. M., & Zoumpourlis, V. (2021). Protective role of taurine against oxidative stress (Review). *Molecular medicine reports*, *24*(2), 605. https://doi.org/10.3892/mmr.2021.12242

Li, X., Li, C., Zhang, W., Wang, Y., Qian, P., & Huang, H. (2023). Inflammation and aging: signaling pathways and intervention therapies. *Inflammation and Aging: Signaling Pathways and Intervention Therapies*, *8*(1). https://doi.org/10.1038/s41392-023-01502-8

Hu, Q., Peng, J., Jiang, L., Li, W., Su, Q., Zhang, J., Li, H., Song, M., Cheng, B., Xia, J., & Wu, T. (2020). Metformin as a senostatic drug enhances the anticancer efficacy of CDK4/6 inhibitor in head and neck squamous cell carcinoma. *Cell Death & Disease*, *11*(10). https://doi.org/10.1038/s41419-020-03126-0

Jiao, Y., Williams, A., & Wei, N. (2022). Quercetin ameliorated insulin resistance via regulating METTL3-mediated N6-methyladenosine modification of PRKD2 mRNA in skeletal muscle and C2C12 myocyte cell line. *Nutrition, metabolism, and cardiovascular diseases : NMCD*, *32*(11), 2655–2668. https://doi.org/10.1016/j.numecd.2022.06.019

Cheng, L., Zhang, X., Huang, Y.-Z., Zhu, Y.-L., Xu, L.-Y., Li, Z., Dai, X.-Y., Shi, L., Zhou, X.-J., Wei, J.-F., & Ding, Q. (2021). Metformin exhibits antiproliferation activity in breast cancer via miR-483-3p/METTL3/m6A/p21 pathway. *Oncogenesis*, *10*(1). https://doi.org/10.1038/s41389-020-00290-y

Bogdanova, D. A., Kolosova, E. D., Pukhalskaia, T. V., Levchuk, K. A., Demidov, O. N., & Belotserkovskaya, E. V. (2024). The Differential Effect of Senolytics on SASP Cytokine Secretion and Regulation of EMT by CAFs. *International journal of molecular sciences*, *25*(7), 4031. https://doi.org/10.3390/ijms25074031

Sun, Y., Gong, W., & Zhang, S. (2023). METTL3 promotes colorectal cancer progression through activating JAK1/STAT3 signaling pathway. *Cell Death and Disease*, *14*(11). https://doi.org/10.1038/s41419-023-06287-w

Zheng, W., Wang, M., Chai, X., Pan, F., Xu, M., Wang, Y., Lan, L., Hu, F., Zhang, Z., & Chen, Z. (2023). Targeted metabolomics analysis of nucleosides and the identification of biomarkers for colorectal adenomas and colorectal cancer. *Frontiers in Molecular Biosciences*, *10*. https://doi.org/10.3389/fmolb.2023.1163089

Wu, Y., Li, L., Wang, L., Zhang, S., Zeng, Z., Lu, J., Wang, Z., Zhang, Y., Zhang, S., Li, H., & Chen, T. (2024). m1A regulator-mediated methylation modification patterns correlated with autophagy to predict the prognosis of hepatocellular carcinoma. *BMC Cancer*, *24*(1). https://doi.org/10.1186/s12885-024-12235-4

Sakai, Y., Kimura, S., & Suzuki, T. (2019). Dual pathways of tRNA hydroxylation ensure efficient translation by expanding decoding capability. *Nature Communications*, *10*(1). https://doi.org/10.1038/s41467-019-10750-8

Cheng, W., Gao, A., Lin, H., & Zhang, W. (2022). Novel roles of METTL1/WDR4 in tumor via m7G methylation. *Molecular Therapy - Oncolytics*, *26*, 27–34. https://doi.org/10.1016/j.omto.2022.05.009

Ying, X., Liu, B., Yuan, Z., Huang, Y., Chen, C., Jiang, X., Zhang, H., Qi, D., Yang, S., Lin, S., Luo, J., & Ji, W. (2021). METTL1-m[7]G-EGFR/EFEMP1 axis promotes the bladder cancer development. *Clinical and Translational Medicine*, *11*(12). https://doi.org/10.1002/ctm2.675

Songe-Møller, L., van den Born, E., Leihne, V., VågbøC. B., Kristoffersen, T., Krokan, H. E., Kirpekar, F., FalnesP. Ø., & Klungland, A. (2010). Mammalian ALKBH8 Possesses tRNA Methyltransferase Activity Required for the Biogenesis of Multiple Wobble Uridine Modifications Implicated in Translational Decoding. *Molecular and Cellular Biology*, *30*(7), 1814–1827. https://doi.org/10.1128/mcb.01602-09

Lee, M. Y., Leonardi, A., Begley, T. J., & Melendez, J. A. (2020). Loss of epitranscriptomic control of selenocysteine utilization engages senescence and mitochondrial reprogramming☆. *Redox Biology*, *28*, 101375. https://doi.org/10.1016/j.redox.2019.101375

Xiong, Q.-P., Li, J., Li, H., Huang, Z.-X., Dong, H., Wang, E.-D., & Liu, R.-J. (2023). Human TRMT1 catalyzes m2G or m22G formation on tRNAs in a substrate-dependent manner. *Science China Life Sciences*, *66*(10), 2295–2309. https://doi.org/10.1007/s11427-022-2295-0

Nombela, P., Miguel-López, B., & Blanco, S. (2021). The role of m6A, m5C and Ψ RNA modifications in cancer: Novel therapeutic opportunities. *Molecular Cancer*, *20*(1). https://doi.org/10.1186/s12943-020-01263-w
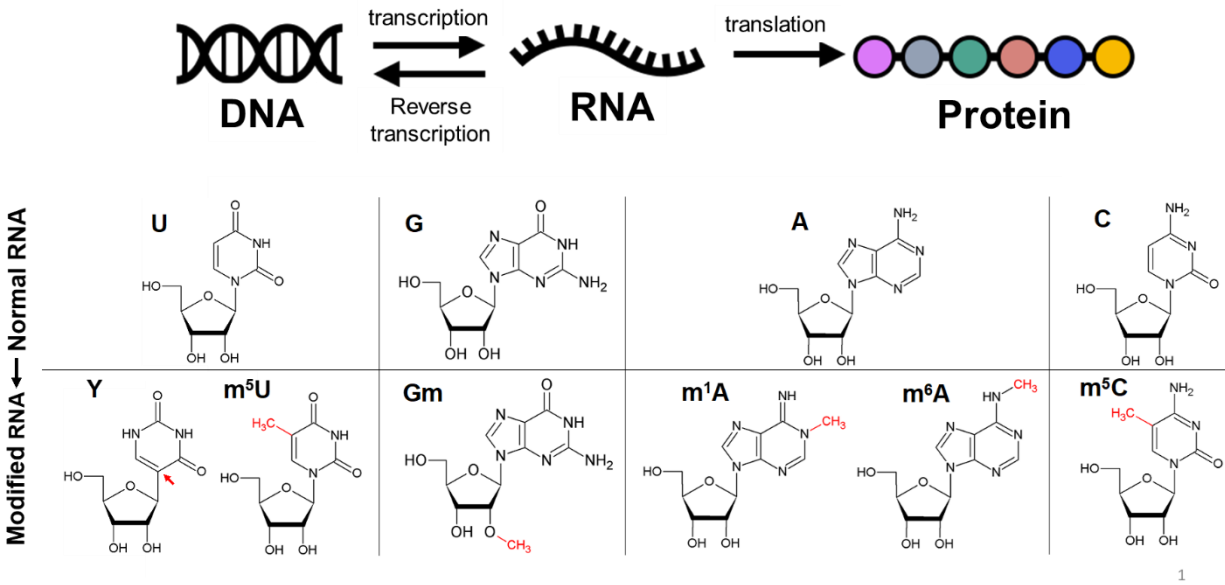
9.Figures

Figure 1. The Central Dogma. Genetic information flows from DNA to RNA to protein. During

transcription, mRNA is synthesized from DNA. During translation, mRNA codes for proteins that

are synthesized at the ribosome. Normal RNA can be modified, where uracil (U) is modified to

m5U, guanine (G) is modified to Gm, adenine (A) is modified to m1A or m6A, and cytosine (C)

is modified to m5C.
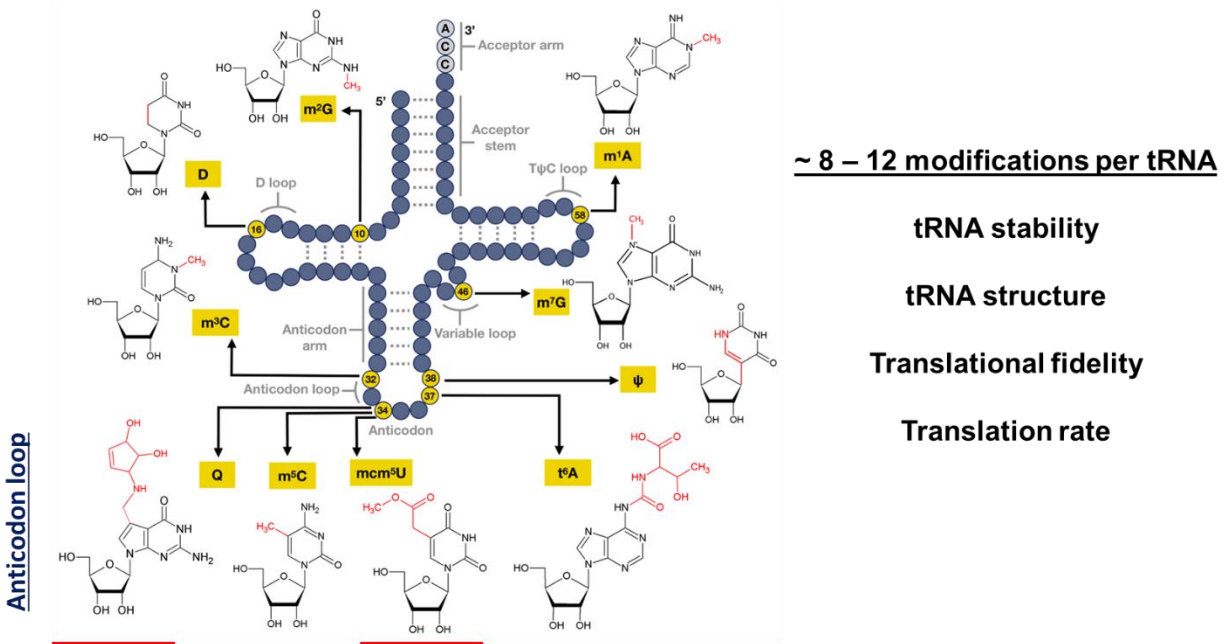
Figure 2. RNA Modifications can Regulate Codon-Anticodon Interactions. There are 8 – 12 modifications per tRNA, and these modifications influence the stability of tRNA, the structure of tRNA, translation fidelity, and the rate of translation The two-dimensional cloverleaf model of tRNA is comprised of three loops. The bottom loop is composed of anticodons, and it binds complementary to mRNA codons. A three-nucleotide acceptor site is present at the 3' end, which includes a free –OH group. Specific tRNA's will bind to specific amino acids through the acceptor stem.
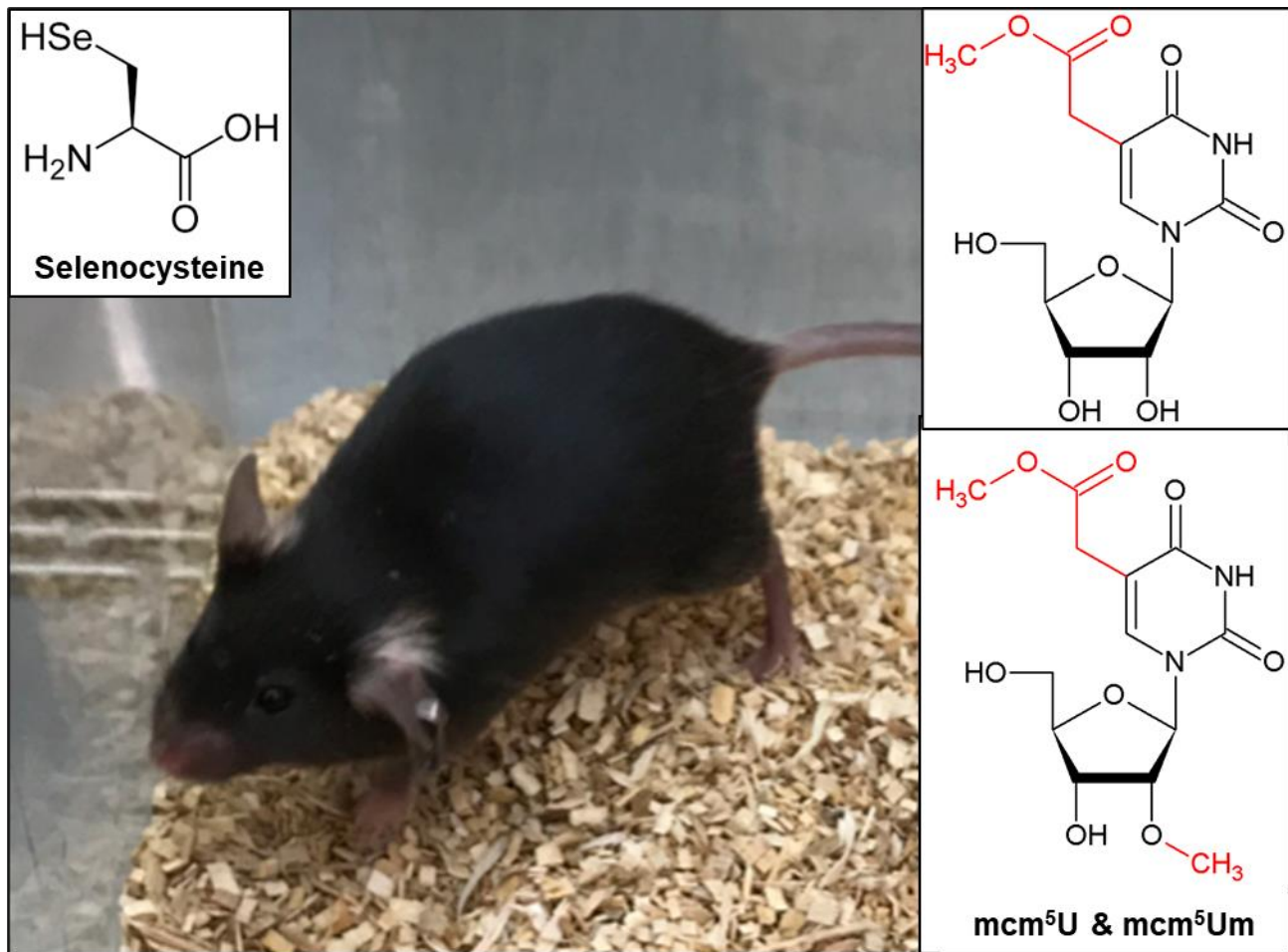
Figure 3. Epitranscriptomic Control of Selenocysteine Translation in Mice: The Wobble U Writer ALKBH8. ALKBH8 is a tRNA methyltransferase that methylates the wobble uridine to mcm5U (5-methoxycarbonylmethyluridine) and mcm5Um (5-methoxycarbonylmethyl-2′-O-methyluridine). These are wobble uridines used to translate selenocysteine codons. Both mcm5U and mcm5Um promote UGA-stop codon recoding which is needed to incorporate selenocysteine. These tRNA modifications increase due to ROS stress to improve selenocysteine translation, which contains GPX and TRXR enzymes.

A

WT MEF Dose Response Curve

n=3
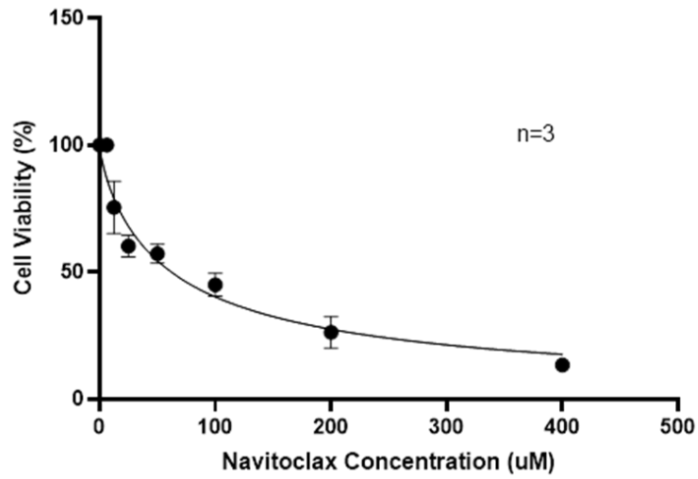
LD20 = 11.69 uM
LD4 = 1.25 uM

B

WT MEF Dose Response Curve

n=3

LD20 = 59.81 uM
LD4 = 9.55 uM

WT MEF Dose Response Curve

C

Cell Viability (%) vs Metformin Concentration (mM)

n=3
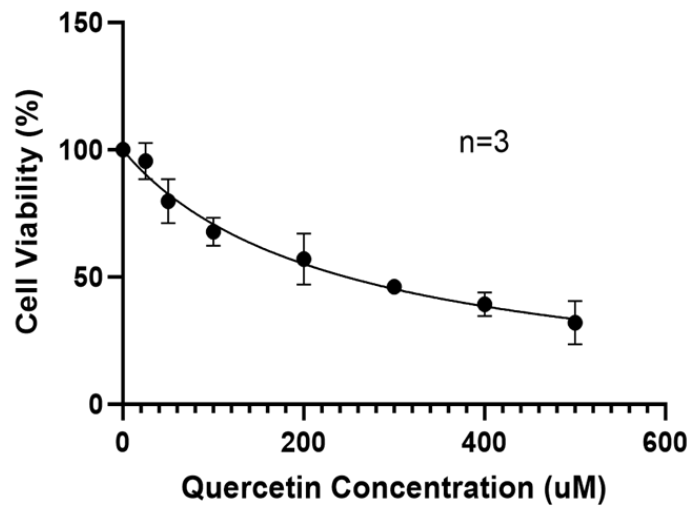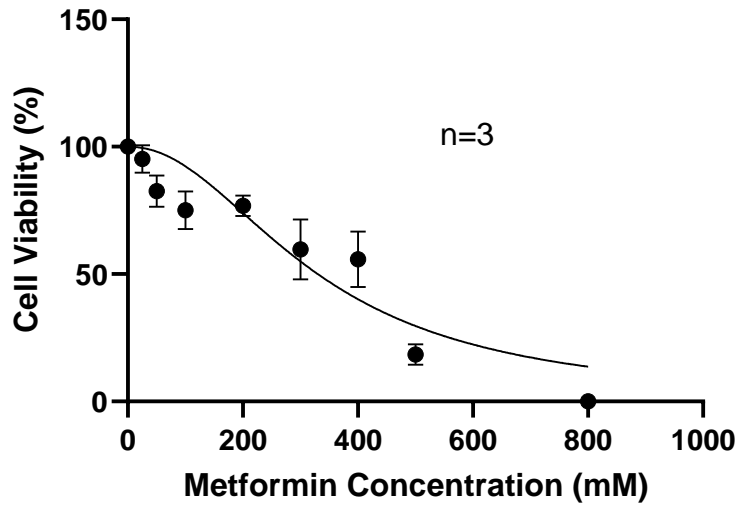
LD20 = 169.89 mM
LD4 = 71.90 mM

Senescent IMR-90 Dose Response Curve

D

Cell Viability (%) vs Navitoclax Concentration (uM)

n = 3
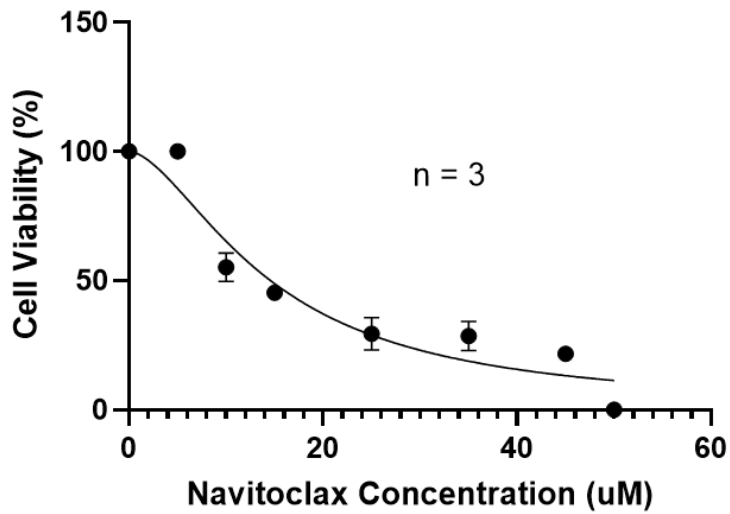
LD20 = 6.37 uM
LD4 = 2.18 uM

Figure 4. Dose Response Curves and LD_4 and LD_{20} Values. WT MEFs were seeded on a 12-well plate and seeded for 24 hours at 37 º C, 5% CO2. MEFs were treated with Navitoclax (**A**), Quercetin (**B**), and Metformin (**C**) in untreated medium for one hour at 37 º C, 5% CO2. After one-hour, untreated medium was replaced with treated medium and incubated for 24 hours at 37 º C, 5% CO2. After 24 hours, the cells were trysponized and centrifuged. The pellets were resuspended in medium, and trypan blue was used for cell counting to obtain an LD20 and an LD4 value. Senescent IMR-90 fibroblasts were seeded on a 12-well plate and seeded for 24 hours at 37 º C, 5% CO2. Senescent IMR-90 fibroblasts were treated with navitoclax (**D**) in untreated medium for one hour at 37 º C, 5% CO2. After one-hour, untreated medium was replaced with treated medium and incubated for 24 hours at 37 º C, 5% CO2. After 24 hours, the cells were trysponized and centrifuged. The pellets were resuspended in medium, and trypan blue was used for cell counting to obtain an LD_{20} and an LD_4 value.
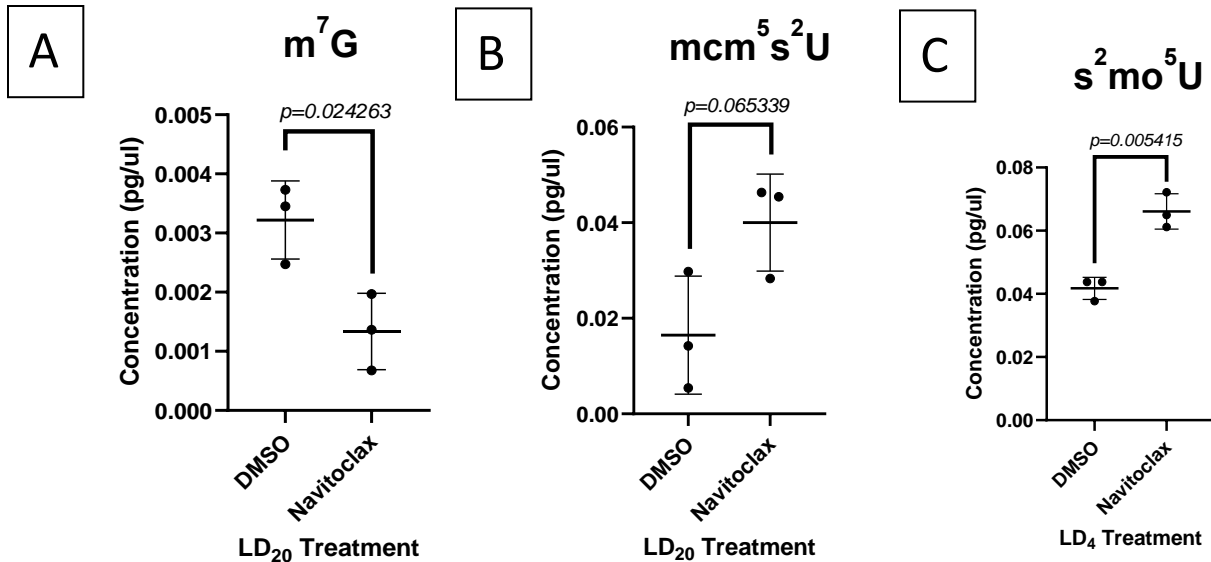
Figure 5. **m7G Decreases in Response to the LD$_{20}$ Treatment of Navitoclax, mcms2U Increases in Response to the LD$_{20}$ Treatment of Navitoclax, and s2mo5U Increases in Response to the LD$_{4}$ Treatment of Navitoclax in WT MEFs.** The unpaired parametric t-test analysis showed there was a significance in m7G between the Navitoclax t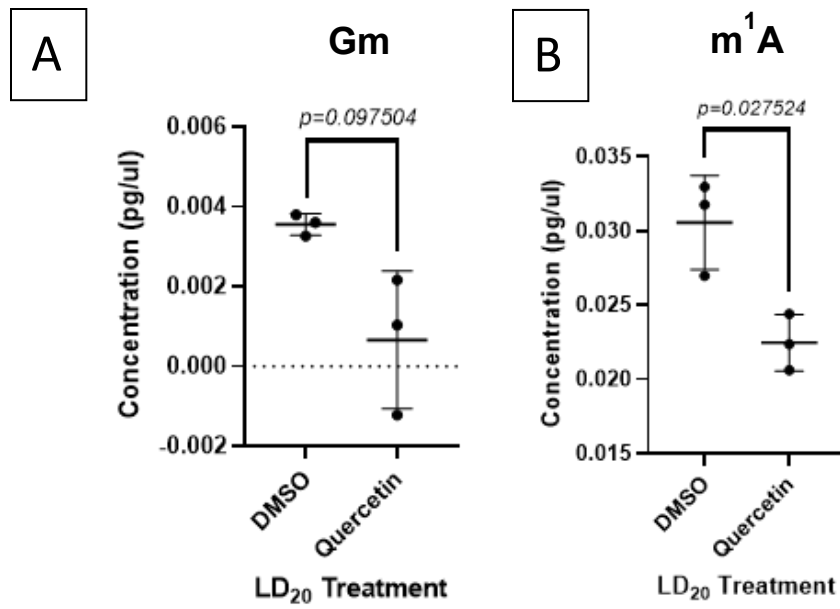reated group and the control group (**A**) (DMSO) (p = 0.024263). The unpaired parametric t-test analysis showed there was a significance in mcm5s2U between the Navitoclax treated group and the control group (**B**) (DMSO) (p = 0.065339). The unpaired parametric t-test analysis showed there was a significance in s2mo5U between the Navitoclax treated group and the control group (**C**) (DMSO) (p = 0.005415).

Figure 6. **Gm and m^{1}A Decrease in Response to the LD20 Treatment of Quercetin in WT MEFs.**

The unpaired parametric t-test analysis showed there was a significance in Gm between the Quercetin treated group and the control group (**A**) (DMSO) (p = 0.097504). The unpaired parametric t-test analysis showed there was a significance in m^{1}A between the Quercetin treated group and the control group (**B**) (DMSO) (p = 0.027524).
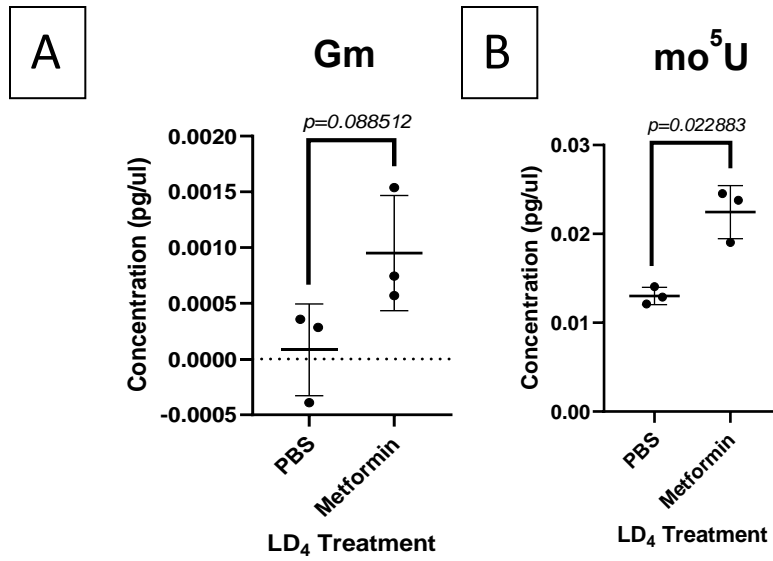
Figure 7. Gm and mo[5]U Increase in Response to the LD₄ Treatment of Metformin in WT

MEFs. The unpaired parametric t-test analysis showed there was a significance in Gm between the Metformin treated group and the control group (**A**) (DMSO) (p = 0.88512). The unpaired parametric t-test analysis showed there was a significance in mo[5]U between the Metformin treated group and the control group (**B**) (DMSO) (p = 0.022883).
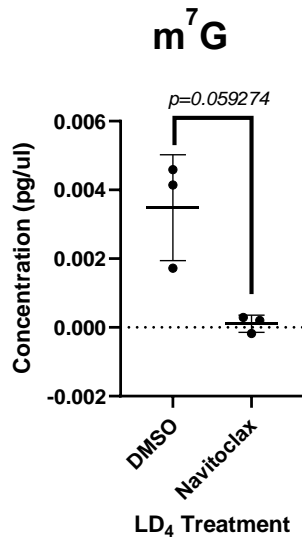
Figure 8. m^{7}G Decreases in Response to the LD$_4$ Treatment of Navitoclax in Senescent IMR-90s. The unpaired parametric t-test analysis showed there was a significance in m^{7}G between the Navitoclax treated group and the control group (DMSO) (p = 0.059274).
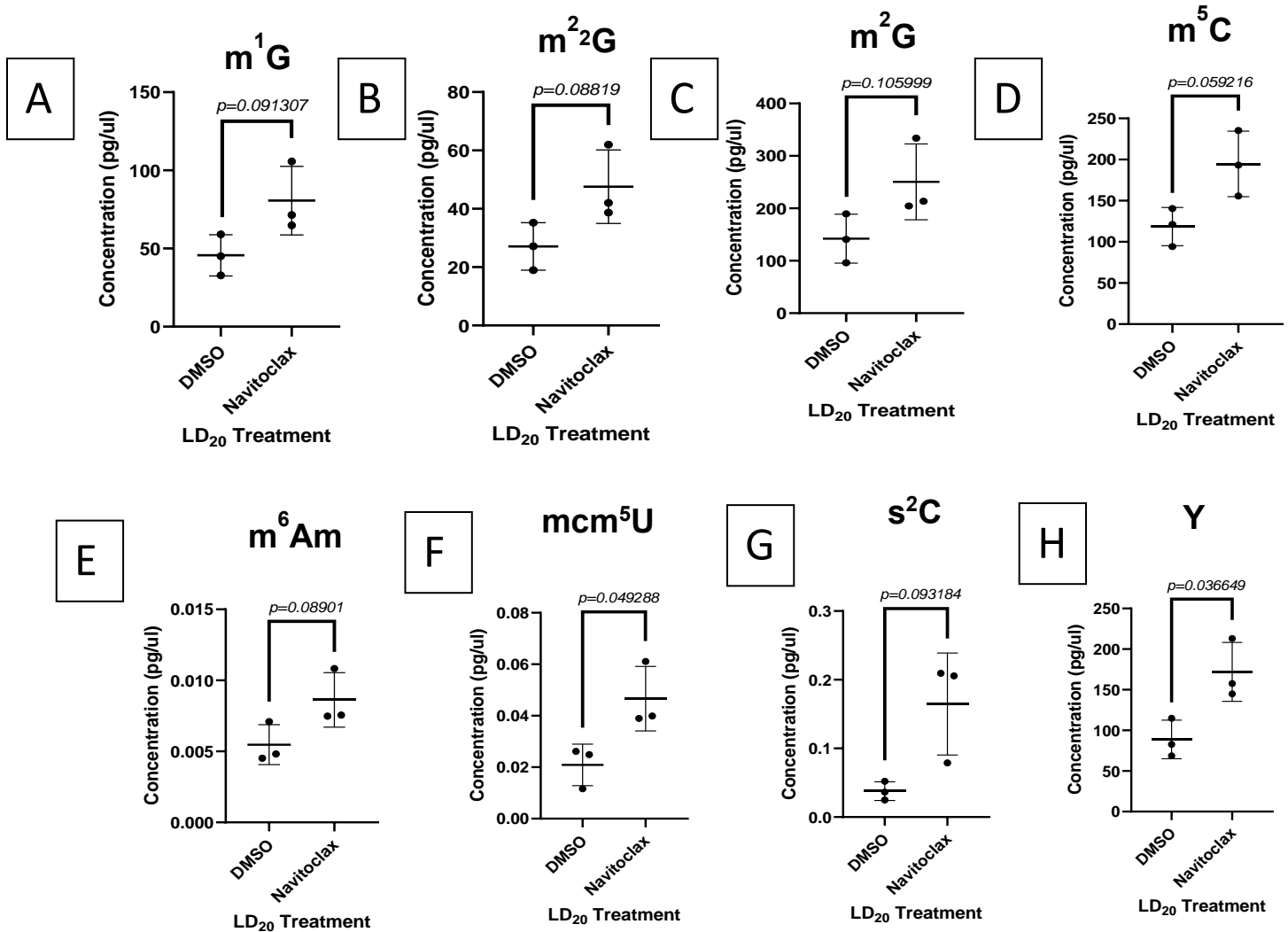
Figure 9. m^1G, m^2_2G, m^2G, m^5C, m^6Am, mcm^5U, s^2C, and Y Increase in Response to the LD_{20} Treatment of Navitoclax in Senescent IMR-90s. The unpaired parametric t-test analysis showed there was a significance in m^1G between the Navitoclax treated group and the control group (**A**) (DMSO) (p = 0.091307). The unpaired parametric t-test analysis showed there was a significance in m^2_2G between the Navitoclax treated group and the control group (**B**) (DMSO) (p = 0.08819). The unpaired parametric t-test analysis showed there was a significance in m^2G between the Navitoclax treated group and the control group (**C**) (DMSO) (p = 0.105999). The unpaired parametric t-test analysis showed there was a significance in m^5C between the Navitoclax treated group and the control group (**D**) (DMSO) (p = 0.059216). The unpaired parametric t-test analysis showed there was a significance in m^6Am between the Navitoclax treated group and the control group (**E**) (DMSO) (p = 0.08901). The unpaired parametric t-test analysis showed there was a significance in mcm^5U between the Navitoclax treated group and the control group (**F**) (DMSO) (p = 0.049288). The unpaired parametric t-test analysis showed there was a significance in s^2C between the Navitoclax treated group and the control group (**G**) (DMSO) (p = 0.093184). The unpaired parametric t-test analysis showed there was a significance in Y between the Navitoclax treated group and the control group (**H**) (DMSO) (p = 0.036649).
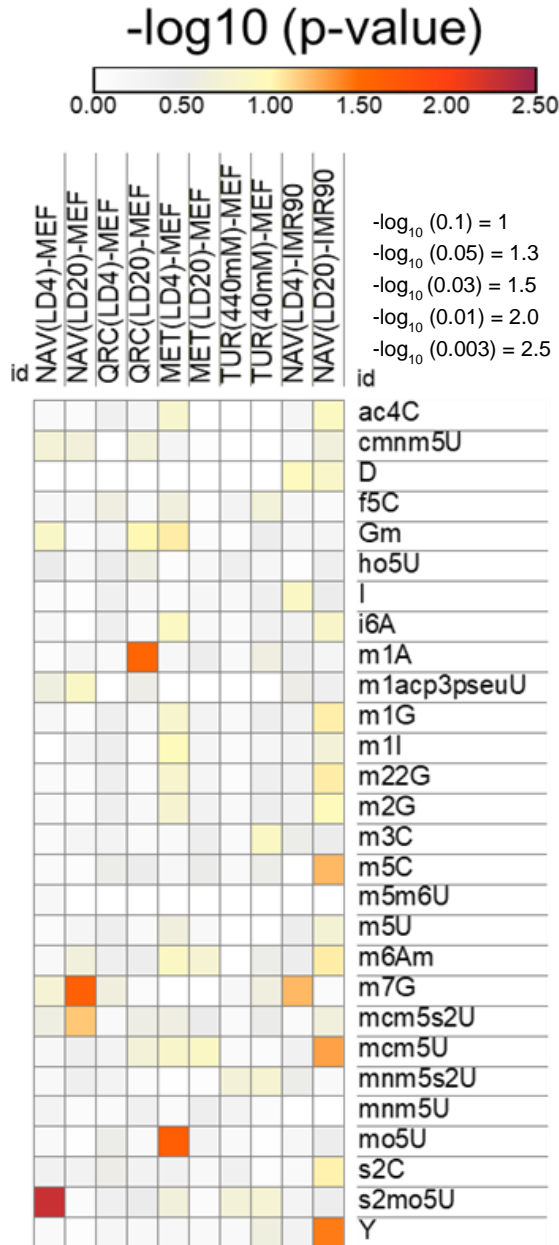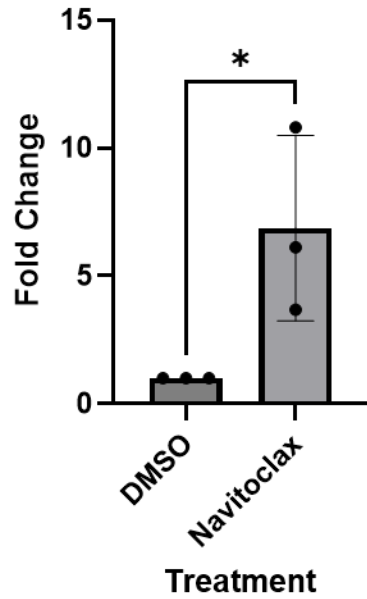
Figure 10. tRNA Modification Analysis of WT MEFs and Senescent IMR-90s Treated with the LD$_4$ and LD$_{20}$ Values of Senolytics and Senomorphs. The list of tRNA modifications were obtained from LC-MS/MS analysis. The list of tRNA modifications are included for all -log$_{10}$(p-value); (0.1, 0.05, 0.03, 0.01, 0.003).
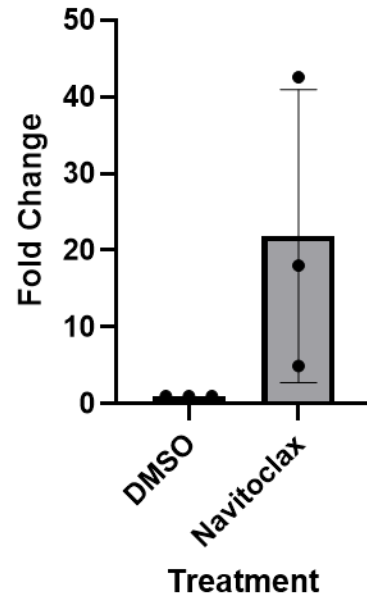
Figure 11. LD$_4$ Treatment of Navitoclax Upregulates IL-8 Expression in Senescent IMR-90 Fibroblasts. The unpaired parametric t-test showed there was significance between the navitoclax treated group and the control group (DMSO) in the LD$_4$ (p = 0.04) (**A**), but not the LD$_{20}$ (p = 0.82) (**B**).
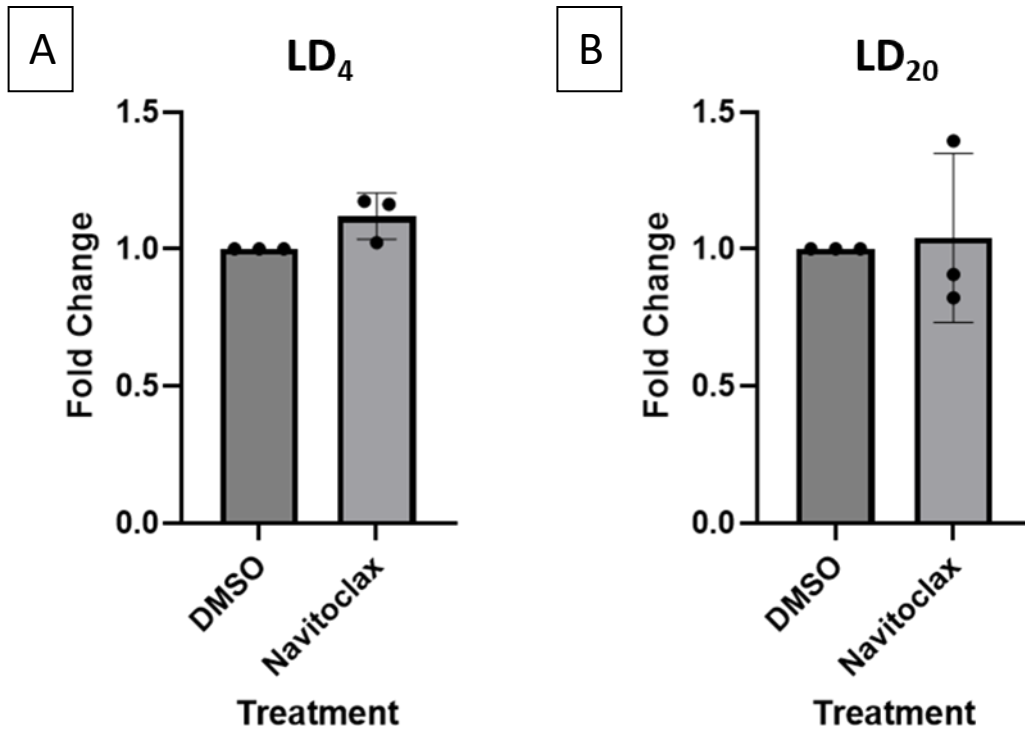
Figure 12. LD$_4$ and LD$_{20}$ Treatments of Navitoclax does not Affect IL-6 Expression in Senescent IMR-90 Fibroblasts. The unpaired parametric t-test showed there was insignificance between the navitoclax treated group and the control group (DMSO) in the LD$_4$ (p = 0.7212) (**A**) and the LD$_{20}$ (p = 0.8077) (**B**).